

# DAMAGE ASSESSMENT IN STEEL STRUCTURES SUBJECTED TO SEVERE EARTHQUAKES

H. Krawinkler (I)

Presenting Author: H. Krawinkler

## SUMMARY

This paper presents an experimental-analytical approach to seismic performance assessment. A simple cumulative damage model is employed to account for the effects of all damaging cycles on strength deterioration. This damage model contains structural performance parameters as well as seismic response parameter. An experimental approach is used to determine the performance parameters of steel components. The seismic response parameters of the damage model are determined from a statistical study. The dependence of cumulative damage on the seismic response parameters is discussed and conclusions are drawn on the feasibility of performance assessment by means of cumulative damage models.

## INTRODUCTION

The study discussed in this paper is concerned with the seismic performance assessment of components of steel structures. The term performance is used here to denote closeness to failure, where failure is defined as the attainment of an unacceptable level of deterioration in resistance. Disregarding the problem of global buckling, deterioration and failure in steel components is usually a consequence of localized phenomena, such as local buckling, lateral torsional buckling, weld fracture, or crack propagation at reduced cross sections (e.g., net section at a bolt line).

Two common modes of deterioration and failure are illustrated in Fig. 1. In one mode [Fig. 1(a)], no noticeable deterioration is observed for several cycles and then deterioration occurs at a very fast rate. The deterioration range covers only a small portion of the useful life of the component and usually can be neglected. Thus, the onset of noticeable deterioration can be considered as the instance of failure. In the other mode [Fig. 1(b)], the deterioration threshold is small but deterioration occurs at a slow rate for several cycles. Here, a significant portion of the useful life may be spent in the deterioration range.

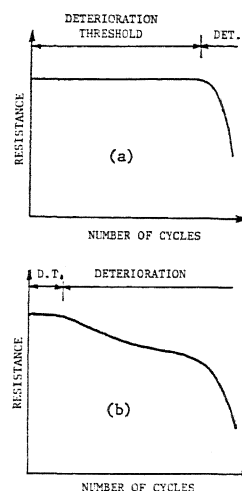


Fig. 1 Modes of Deterioration

The aspect common to both failure modes is that deterioration is always a consequence of the cumulative effect of all cycles to which the component is subjected. In order to assess the seismic performance it is necessary, therefore, to account for this cumulative effect which depends on the cyclic load--deformation characteristics of the component as well as on the magnitudes of all cycles which the component experiences in an earthquake.

(I) Professor of Civil Engineering, Stanford University, California, USA

The objective of this paper is to propose a simple cumulative damage model that can be used for performance evaluation, and to discuss a method that can be employed to obtain statistical information on the number and magnitudes of damaging cycles. The accuracy of the damage models is assessed in an experimental study on two specific failure modes. Detailed information on the studies summarized in this paper can be found in Ref. 1.

#### MODELS FOR PERFORMANCE ASSESSMENT

When a structural component is subjected to cyclic loading, it can be assumed that every cycle, whose magnitude exceeds a certain threshold, will cause microstructural changes that bring the component closer to a state of failure. Although these microstructural changes may not alter visibly the overall response, they constitute damage that accumulates from cycle to cycle. Once the accumulated damage  $D$  exceed a limit value  $\gamma$ , failure will take place. Thus, a general assessment of performance can be expressed as

$$P_f = P[D > \gamma] \quad (1)$$

where  $P_f$  is the probability of failure.

The task at hand is to find a damage function that accounts for cumulative effects of cycles of different magnitudes. For steel components subjected to seismic excitations, the classical low-cycle fatigue approach appears to be appropriate. This approach is based on the hypothesis that for constant amplitude cycling the number of cycles to failure,  $N_f$ , can be related to a plastic deformation range of the cycle,  $\Delta\delta_p$ , by an equation of the type

$$N_f = C^{-1}(\Delta\delta_p)^{-c} \quad (2)$$

where  $C$  and  $c$  are structural performance parameters. The plastic deformation range is defined in Fig. 2 and the deformation quantity to be used depends on the failure mode under study. Using the hypothesis of linear damage accumulation (Miner's rule), the damage per cycle is equal to  $1/N_f$ , and the accumulated damage after  $N$  cycles with different ranges  $\Delta\delta_{pi}$  can be expressed as

$$D = \sum_{i=1}^N \frac{1}{N_{fi}} = C \sum_{i=1}^N (\Delta\delta_{pi})^c \quad (3)$$

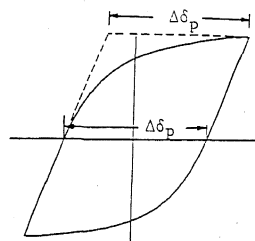


Fig. 2 Plastic Def. Range  $\Delta\delta_p$

This equation is the simplest damage model that can be proposed for structural components. The use of Miner's rule has the shortcomings that mean effects and sequence effects are not considered. Although these effects may be of some importance, they are neglected in this discussion in order to keep the damage model as simple as possible. If Miner's rule were valid, a damage value of one would constitute failure, but because of the shortcomings of Miner's rule the limit value of damage that constitutes failure should be treated as a random variable  $\gamma$ .

Referring to Eq. (1), the probability of component failure can now be expressed as

$$P_f = P[D > \gamma] = P\left[C \sum_{i=1}^N (\Delta\delta_{pi})^c > \gamma\right] \quad (4)$$

This equation, which is graphically illustrated in Fig. 3, would permit a probabilistic assessment of component failure provided that the uncertainties in all the variables contained in the equation can be evaluated and a probabilistic distribution of  $D$  can be formulated. No attempts are made here to pursue this probabilistic formulation because of insufficient data on the uncertainties in the variables.

The purpose of the following discussion is to assess the validity of the simple damage model expressed by Eq. (3) and to examine how the structural performance parameters  $C$  and  $c$  can be determined through experimental research.

#### EXPERIMENTAL STUDY ON COMPONENT PERFORMANCE

Two series of experiments were performed on steel beam specimens in order to assess the damage model expressed by Eq. (3). Ten identical specimens were used in each series. The histories imposed on the specimens included constant deflection amplitude cycling and variable deflection amplitude cycling. The constant amplitude tests were used to determine the structural performance parameters  $C$  and  $c$  and the variable amplitude tests were used to examine the accuracy of the damage models.

The test specimens were cantilever beams made of small hot rolled A36 steel sections welded to column stubs as shown in Fig. 4. Different W sections were used in the two series to study two distinctly different modes of deterioration and failure, namely, a crack propagation mode and a local buckling mode. The cantilever beams were loaded at the tip, with tip deflection being the control parameter for the loading history.

#### Crack Propagation at Weldments

In the B1 specimens, crack propagation at the toe of the beam flange to column flange weld (see Fig. 5) was the cause of deterioration and failure. In all specimens, one or several small cracks near the beam flange centerline were observed very early in the loading history. The small cracks joined soon and a single crack propagated through the heat affected zone (HAZ) of the flange. When the crack size (depth) exceeded half the flange thickness, fracture occurred through the flange thickness and the through-crack propagated rapidly across the flange.

The crack growth through the flange thickness did not lead to a noticeable deterioration in the global load--deflection response. But rapid deterioration occurred once a through-crack was formed and the crack propagated across the flange. Thus, the deterioration and failure mode for crack propagation is of the type illustrated in Fig. 1(a). In this case, only the deterioration threshold range needs to be

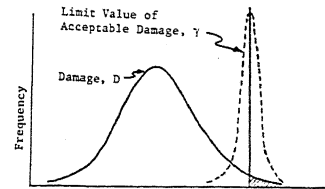
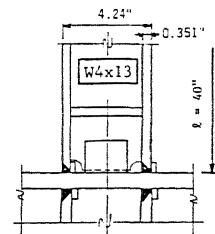
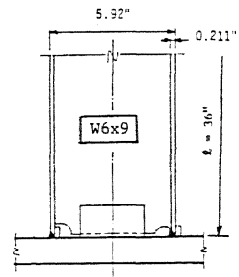


Fig. 3 Probabilistic Description of Damage and its Limit Value



(a) B1 Specimens



(b) B2 Specimens

Fig. 4 Details of Test Specimens

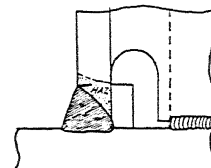


Fig. 5 Crack at Weld Toe

modeled and failure can be assumed to coincide with the occurrence of a through-crack in the flange. Two approaches can be used to model this deterioration threshold range.

In the low-cycle fatigue approach the structural performance parameters  $C$  and  $c$  can be determined directly from constant amplitude tests and utilizing Eq. (2). Taking the measured plastic strain range close to the crack,  $\Delta\epsilon_p$ , as the controlling deformation parameter, the constant amplitude tests give the results shown in Fig. 6. There is an evident scatter around the regression line, indicating that at least one of the performance parameters should be treated as a random variable. Accepting the validity of Miner's rule, accumulation of damage under variable amplitude cycling can be estimated from Eq. (3).

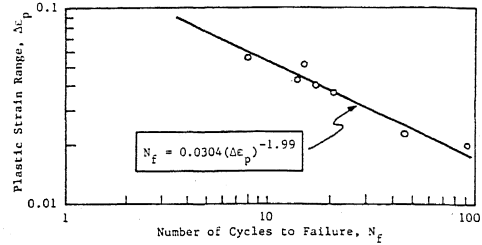


Fig. 6 Results of Constant Amplitude Tests

An alternative approach is to use fracture mechanics concepts to predict damage accumulation. In this approach, an initial crack of size  $a_0$  is assumed to exist in the virgin specimen because of the presence of imperfections at the weld toe, and crack growth through the flange is predicted from a crack growth rate model. Crack size measurements obtained from striations on the fracture surface showed that for constant amplitude cycling the crack growth rate per cycle,  $da/dN$ , and the plastic strain amplitude,  $\Delta\epsilon_p$ , can be related by an equation of the form

$$\frac{da}{dN} = \alpha(\Delta\epsilon_p)^\beta \quad (5)$$

where  $a$  is the crack size and  $\alpha$  and  $\beta$  are fracture mechanics parameters. The crack growth rate model fitted to the data of six constant amplitude tests is shown in Fig. 7. This figure shows that the data points deviate very little from the regression line, indicating that the scatter is negligible and  $\alpha$  and  $\beta$  need not be treated as random variables.

Assuming that the initial crack size  $a_0$  is known, the number of cycles to failure for constant amplitude cycling can be evaluated by integrating the crack growth rate model from  $a_0$  to a critical crack size  $a_c$ , resulting in the expression

$$N_f = \alpha^{-1} \ln \frac{a_c}{a_0} (\Delta\epsilon_p)^{-\beta} \quad (6)$$

This expression is identical in form to Eq. (2). Thus, the low-cycle fatigue approach and the fracture mechanics approach result in identical formulations for life predictions although the two approaches are based on distinctly different concepts. Moreover, the use of the crack growth rate model given by Eq. (5) for cycles with variable amplitudes is equivalent to the use of Miner's rule in the damage model expressed by Eq. (3). Thus, this damage model can be expressed in terms of fracture mechanics parameters as follows:

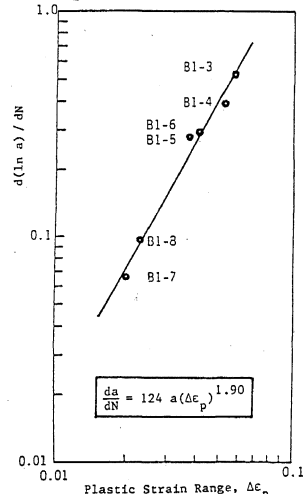


Fig. 7 Crack Growth Rate Model

$$D = \sum_{i=1}^N \frac{1}{N_{fi}} = \alpha \left( \ln \frac{a_c}{a_o} \right)^{-1} \sum_{i=1}^N (\Delta \epsilon_{pi})^\beta$$

The advantage of the formulation given by this equation is that physical crack sizes are employed to determine the structural performance parameter  $C$ . For the component tested in this study, the critical crack size  $a_c$  was approximately equal to half the flange thickness and did not vary much between specimens. Most of the uncertainty in life predictions came from the initial crack size  $a_o$  which depends on the initial imperfections at the weld toe. Rather than attempting to measure  $a_o$ , which is an impossible and futile task (because of irregular crack growth in the early stages), it was decided to predict  $a_o$  for each test from Eq. (6), using the experimental information on the parameters. The mean value and standard deviation of  $a_o$  were found to be 0.00163 in. and 0.00123 in., respectively. This indicates a large scatter in initial crack size which explains the significant scatter in observed lives evident in Fig. 6. Thus, for a crack propagation mode of failure the structural performance parameter  $C$  should be taken as a random variable with the major source of randomness attributed to the initial crack size.

Equation (5) was utilized to predict the crack growth in a test with variable amplitude cycling. The history for this test was a realistic seismic response history that was applied repeatedly to the specimen. The results of the experiment and the analytical predictions are shown in Fig. 8. The two predicted crack growth curves show that the initial crack size has a considerable effect on life prediction. Since the initial crack size of the test specimen is not known, a definite conclusion cannot be drawn from this figure, but it is very likely that the life prediction based on the crack growth rate model is conservative.

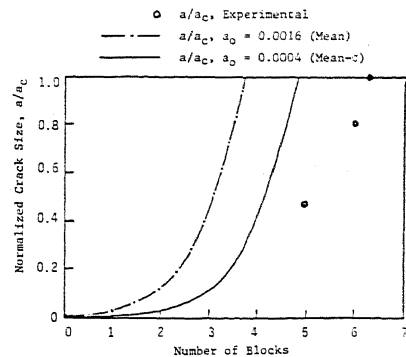


Fig. 8 Crack Growth Predictions and Experimental Results

#### Local Buckling in Beam Flanges

In the B2 specimens [Fig. 4(b)], local flange buckling was the cause of deterioration and failure. The deterioration mode was of the type shown in Fig. 1(b). In all constant deflection amplitude tests the peak load deteriorated in a manner that can be represented closely by the straight line diagram shown in Fig. 9. The first two deterioration ranges were caused by local buckling whereas the rapid deterioration at the end (range III) was caused by crack propagation at the beam flange weld.

The slopes of the lines shown in Fig. 9 represent the deterioration rates per cycle. If these slopes are plotted in a log-log scale against the plastic rotation range for each constant amplitude test, the results shown in Fig. 10 are obtained. Straight correlation lines match well with the data points in

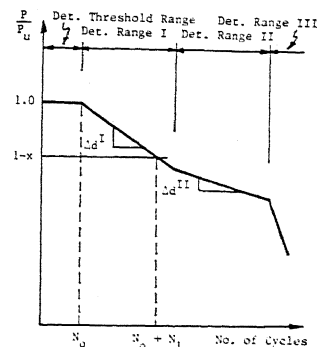


Fig. 9 Deterioration Ranges for Local Buckling Mode

deterioration range I (solid line) and less satisfactorily with the data points in deterioration range II (dashed line). Thus, it can be postulated that, at least in range I, strength deterioration per cycle,  $\Delta d$ , and plastic rotation range,  $\Delta\theta_p$ , can be related by an expression of the type

$$\Delta d = A(\Delta\theta_p)^a \quad (8)$$

If we denote with "x" the limit value of acceptable deterioration that constitutes failure, the number of cycles spent in the deterioration range,  $N_1$ , can be calculated as

$$N_1 = \frac{x}{\Delta d} = x A^{-1}(\Delta\theta_p)^{-a} \quad (9)$$

This expression is again of the form given by Eq. (2). Presuming that also the deterioration threshold range can be modeled by a similar expression, the number of cycles to failure is given by

$$N_f = N_0 + N_1 = C_0^{-1}(\Delta\theta_p)^{-c_0} + x A^{-1}(\Delta\theta_p)^{-a} \quad (10)$$

where  $N_0$  is the number of cycles spent in the deterioration threshold range.

In order to utilize a damage model of the type given by Eq. (3) for variable amplitude cycling, two approaches can be used. One is to use, in series, two separate damage models for the deterioration threshold range and for the deterioration range. The other is to use an average deterioration rate for both ranges. In this case the damage model would take the form

$$D = \sum_{i=1}^N \frac{1}{C_0^{-1}(\Delta\theta_{pi})^{-c_0} + x A^{-1}(\Delta\theta_{pi})^{-a}} \quad (11)$$

This model is only approximate but has the advantage that the use of two separate damage models is avoided.

The accuracy of predicting deterioration with the deterioration rate model given by Eq. (8) (including the deterioration threshold) was examined on a variable amplitude test. The results of the test and the predictions are shown in Fig. 11. The predictions are conservative but quite adequate, particularly when the second deterioration range is included in the model.

#### DETERMINATION OF SEISMIC RESPONSE PARAMETERS

Equations (3) and (4) show that performance assessment requires information on the number of cycles and the magnitudes of the plastic deformation ranges. A pilot study was performed to obtain statistical data on these seismic response parameters. Six California ground motion records were used for this purpose. The records were scaled to a common severity level by matching their spectral shapes to the spectra used in the ATC-3 project (Ref. 2).

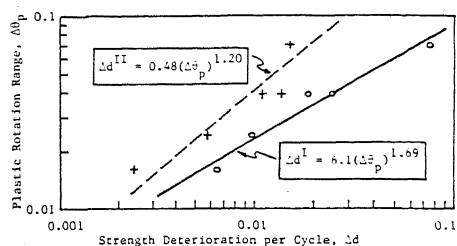


Fig. 10 Deterioration Rate Model

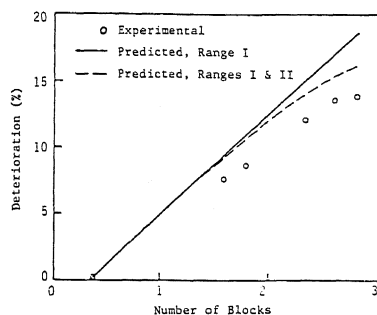


Fig. 11 Experimental and Predicted Deterioration

The scaled records were used to perform time history analyses on single degree of freedom systems. Bilinear nondegrading systems as well as stiffness degrading systems (Clough's model) were used. Systems with different strain hardening ratios  $\alpha$  and different yield levels were investigated. The yield levels were obtained by dividing the smoothened elastic spectral values by a yield level reduction factor  $R$ . In this pilot study only structural systems with a natural period of 0.5 seconds were investigated.

From the time history results the inelastic excursions were isolated, redefined by employing the rain-flow cycle counting method, and ordered in increasing magnitude. This resulted into a series of plastic deformation ranges suitable for low-cycle fatigue damage modeling. It was found that the ordered plastic deformation ranges for each system and record follow approximately a straight line if plotted on a log-normal probability paper. Thus, order statistics was used to combine the data from all six records and to arrive at a representative log-normal distribution of plastic deformation ranges for each structural system.

Numerical data for the log-normal distributions are presented in Ref. 1. A typical result is shown in Fig. 12. This figure illustrates the low frequency of large plastic deformation ranges and the high frequency of small plastic deformation ranges. Because of this high frequency, the cumulative effect of small plastic deformation ranges on damage is not negligible.

The results of a regression analysis of the number of inelastic excursions (half cycles),  $N'$ , and the strong motion duration  $D_{sm}$  are shown in Fig. 13. The correlation coefficients for all four regression lines are greater than 0.95, indicating a strong linear dependence of  $N'$  on  $D_{sm}$ . The effect of the strain hardening ratio  $\alpha$  on  $N'$  was found to be small. The effect of yield level on  $N'$  is moderate for bilinear nondegrading systems and small for stiffness degrading systems.

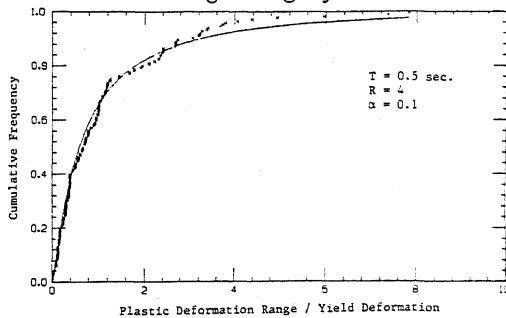


Fig. 12 Typical Log-Normal Distribution of  $\Delta\delta_p/\delta_y$

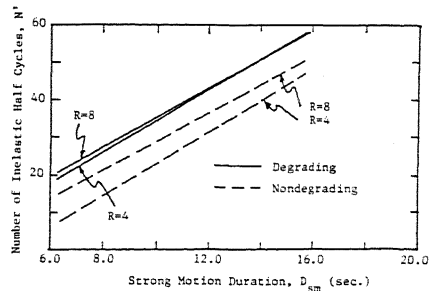


Fig. 13 Regression Lines for  $N'$  versus  $D_{sm}$

The results of this analytical study were utilized to assess the effect of strong motion duration on cumulative damage. For this purpose the damage model given by Eq. (3) was utilized, with the exponent  $c$  taken equal to 2.0. Damage values were normalized with respect to the damage  $\bar{D}$  caused by the maximum plastic deformation range. The results for a specific system are presented in Fig. 14. Shown in this figure are the damage values calculated from the time history results and the corresponding regression line (solid line), as well as the predicted regression line based on the analytical models for the number of inelastic cycles and the log-normal distribution of plastic deformation ranges.

The observed data points show a considerable scatter, but the two regression lines match rather well, indicating that the mathematical models lead to realistic damage predictions. The important conclusion to be drawn from this figure is that cumulative damage depends strongly on the strong motion duration. This demonstrates the need for cumulative damage models in performance assessment. The use of a single parameter for performance assessment, such as the conventional ductility ratio, will not capture the cumulative effects and may be misleading.

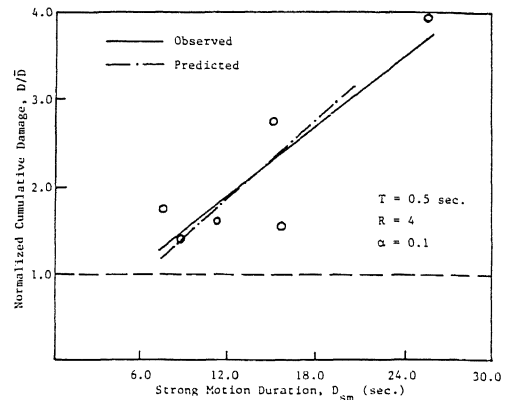


Fig. 14 Dependence of Damage on Strong Motion Duration

### CONCLUSIONS

1. The seismic performance of steel components can be evaluated by means of the simple cumulative damage model given by Eq. (3).
2. The damage model contains two structural performance parameters,  $C$  and  $c$ . The coefficient  $C$  depends strongly on the failure mode and on detailing and should be treated as a random variable. The exponent  $c$  is a much more stable parameter and is usually in the order of 1.5 to 2.0.
3. Damage accumulation in a function of the number of inelastic cycles and of the magnitudes of the individual plastic deformation ranges the component will experience in an earthquake.
4. The seismically induced plastic deformation ranges can be described by a log-normal probability distribution.
5. The number of inelastic cycles and the accumulated damage are strongly dependent on the strong motion duration of the ground motion.

### ACKNOWLEDGEMENTS

The research reported in this paper was supported by the National Science Foundation through the Grant CEE-7902616. The graduate students M. Zohrei, B. Lashkari-Irvani and H. Hadidi-Tamjed participated skillfully and diligently in this research.

### REFERENCES

1. Krawinkler, H., Zohrei, M., Lashkari-Irvani, B., Cofie, N., and Hadidi-Tamjed, H., "Recommendations for Experimental Studies on the Seismic Behavior of Steel Components and Materials," John A. Blume Earthquake Engineering Center Report No. 61, Department of Civil Engineering, Stanford University, September 1983.
2. Applied Technology Council, Tentative Provisions for the Development of Seismic Regulations for Buildings, National Bureau of Standards, Special Publication 510, ATC Publication ATC 3-06, June 1978.